



Performance Diagnosis of the Drive Unit for High Speed Motorized Spindle Based on Hidden State Mapping Model

Zhengwei Jia, Liting Fan, Chunxia Zhu, Zhipeng Si and Jizhi Liu

EasyChair preprints are intended for rapid dissemination of research results and are integrated with the rest of EasyChair.

June 29, 2020

Performance Diagnosis of the Drive Unit for High Speed Motorized Spindle Based on Hidden State Mapping Model

Zhengwei Jia¹, Liting Fan¹, chunxia zhu¹, Zhipeng Si¹ and Jizhi Liu¹

1. School of Mechanical Engineering, Shenyang Jianzhu University, Shenyang 110168
E-mail: fanliting@sjzu.edu.cn

Abstract: As the key component of the motorized spindle system, the performance of drive unit will directly affect the processing quality of CNC machine tools. This paper proposed a performance diagnosis method for the drive unit based on hidden state mapping model to prevent the motorized spindle from failure. The hidden state model was obtained by feature extraction of the parameter vectors identified from the dynamic responses to test input signals. The thresholds of performance degradation were determined by the hidden state to evaluate the performance of the drive unit in the motorized spindle system. A simulation case was carried out to verify the feasibility and effectiveness of the proposed model by taking IGBT degradation failure as an example. The results showed that the model parameters extracted from different degradation degrees of IGBT devices can be mapped to hidden state characteristics and used for performance evaluation of the drive unit. The proposed hidden state mapping model can be used in the framework of monitoring the safety and reliability of the drive unit, and lay the foundation for the prognostic and health management of the motorized spindle system.

Key words: Performance Diagnosis, High Speed Motorized Spindle, Drive Unit, Hidden State Mapping

1. introduction

High-end CNC machine tools provide guarantee for the manufacture of high-tech products in my country, it is a processing equipment commonly used in my country's manufacturing industry and basic equipment for manufacturing, widely used in aerospace, automotive and power generation equipment manufacturing industries. The health of the system is used to describe the ability of the entire system to maintain a certain degree of reliability and continue to achieve predetermined goals. Health monitoring is a kind of periodic detection of a certain part of the system parameters or characteristics failure. During the long-term use of the equipment, the phenomenon of aging and wear inside the equipment, the performance of the equipment is degraded. With long-term performance degradation, the device is malfunctioning. In large mission-critical systems, an advanced detection system can continuously assess the health of the system. Production equipment should be regularly evaluated for performance to avoid downtime maintenance.

There are many ways to evaluate performance, the evaluation method introduced in the reference^[1] to determine the evaluation weight, this method can provide a reference for mechanical system performance evaluation and similar problems, but the scale workload is too large, it should cause disgust and confusing judgment experts; reference^[2] describes the method of fuzzy comprehensive evaluation, it has the characteristics of clear results and strong systemicity, and can better solve fuzzy and difficult to quantify problems. It is suitable for solving various non-deterministic problems, but it has strong subjective certainty to the index

weight vector; This article uses the method of system identification performance evaluation, Determine the parameters of the system model by performing system identification on the system in the normal state, identify systems at different stages of degradation. Study the mapping relationship between the geometric distance of the parameter vector and the performance degradation, and evaluate the performance of the current drive system^[3]. Through IGBT performance degradation simulation examples to verify, the result shows: as the degree of performance degradation continues to intensify, the geometric distance of the system parameter vector gradually increases. Confirm the feasibility of this performance evaluation method.

2. High-speed electric spindle drive system simulation design, system identification

2.1 Drive system simulation design

The high-speed electric spindle drive system is a closed-loop system composed of a frequency converter, a spindle motor, and a vector controller. The spindle motor has synchronous motor and asynchronous motor, this design selects asynchronous motor for design analysis. The basic idea of the closed-loop vector control system is to generate the same rotating magnetomotive force as a criterion, The stator alternating current of the asynchronous motor on the static three-phase coordinate system is equivalent to the direct current on the synchronous rotating coordinate system through coordinate transformation, And control them separately, so as to realize the decoupling control of magnetic flux and torque, so as to achieve the control effect of DC motor^[4]. The mathematical model of asynchronous motor on the two-phase synchronous rotating coordinate system includes voltage equation, flux linkage equation and electromagnetic torque equation. They are as follows:

$$\begin{bmatrix} u_{sd} \\ u_{sq} \\ u_{rd} \\ u_{rq} \end{bmatrix} = \begin{bmatrix} R_s + L_s P & -\omega_1 L_s & L_m P & -\omega_1 L_m \\ \omega_1 L_s & R_s + L_s P & \omega_1 L_m & L_m P \\ L_m P & -\omega_1 L_m & R_r + L_r P & -\omega_s L_r \\ \omega_s L_m & L_m P & \omega_s L_r & R_r + L_r P \end{bmatrix} \begin{bmatrix} i_{sd} \\ i_{sq} \\ i_{rd} \\ i_{rq} \end{bmatrix} \quad (1)$$

$$\begin{bmatrix} \psi_{sd} \\ \psi_{sq} \\ \psi_{rd} \\ \psi_{rq} \end{bmatrix} = \begin{bmatrix} L_s & 0 & L_m & 0 \\ 0 & L_s & 0 & L_m \\ L_m & 0 & L_r & 0 \\ 0 & L_m & 0 & L_r \end{bmatrix} \begin{bmatrix} i_{sd} \\ i_{sq} \\ i_{rd} \\ i_{rq} \end{bmatrix} \quad (2)$$

$$T_e = n_p L_m (i_{sq} i_{rd} - i_{sd} i_{rq}) \quad (3)$$

When the two-phase synchronous rotating coordinate system is oriented according to the rotor flux linkage, presence $\psi_{rd} = \psi_r$, $\psi_{rq} = 0$:

$$T_e = n_p \frac{L_m}{L_r} i_{sq} \psi_r \quad (4)$$

$$i_{sd} = \frac{1 + T_r P}{L_m} \psi_r \quad (5)$$

$$\psi_r = \frac{L_m}{1 + T_r P} i_{sd} \quad (6)$$

$$\omega_s = \frac{L_m}{T_r \psi_r} i_{sq} \quad (7)$$

In the formula: ω_1 is the synchronous speed; ω is the rotor speed; ω_s is slip angular velocity; u is the voltage; ψ is flux linkage; i is the current; R is the resistance; L is the inductance; n_p is polar logarithm; T_r is the rotor time constant; $P = \frac{d}{dt}$ is the differential factor. s represents stator; r represents the rotor; d represents d -axis; q represents q -axis; m represents the mutual inductance between the coaxial stator and rotor.

2.1.1 Transformation of three-phase stationary coordinate system and two-phase stationary coordinate system (referred to as 3s/2s transformation)

In the AC motor, the three-phase symmetrical winding with three-phase symmetrical current can generate a spatially rotating magnetic field in the air gap of the motor. Under the condition of constant power, according to the principle of equal magnetic momentum, the space rotating magnetic field generated by the three-phase symmetrical winding can be equivalent with two symmetric windings. The transformation of the three-phase stationary coordinate system and the two-phase stationary coordinate system establishes that the magnetomotive force remains unchanged. The relationship between the voltage, current and magnetomotive force of the three-phase winding and the two-phase winding. Set the current of two symmetrical windings, Current of three-phase symmetrical winding, the transformation relationship between them is:

$$\begin{bmatrix} i_\alpha \\ i_\beta \\ i_0 \end{bmatrix} = \sqrt{\frac{2}{3}} \begin{bmatrix} 1 & -\frac{1}{2} & -\frac{1}{2} \\ 0 & \frac{\sqrt{3}}{2} & -\frac{\sqrt{3}}{2} \\ \frac{1}{\sqrt{2}} & \frac{1}{\sqrt{2}} & \frac{1}{\sqrt{2}} \end{bmatrix} \begin{bmatrix} i_A \\ i_B \\ i_C \end{bmatrix} = C_{3/2} \begin{bmatrix} i_A \\ i_B \\ i_C \end{bmatrix} \quad (8)$$

In formula(1), It is a one-phase zero-sequence component added for inverse transformation. $C_{3/2}$ is 3s/2s transformation matrix.

2.1.2 Transformation between two-phase stationary coordinate system and two-phase rotating coordinate system (referred to as 2s/2r transformation)

The two-phase static winding is connected with a two-phase balanced alternating current to

generate a rotating magnetomotive force. If the two-phase windings are turned up and the rotation angular velocity is equal to the rotation angular velocity of the resultant magnetomotive force, then the two-phase windings are connected with direct current to produce space rotating magnetomotive force. Transformation from a two-phase stationary coordinate system to a two-phase rotating coordinate system, called two-phase rotation-two-phase static transformation, referred to as C transformation. The transformation formula is:

$$\begin{bmatrix} i_\alpha \\ i_\beta \end{bmatrix} = \begin{bmatrix} \cos \varphi & -\sin \varphi \\ \sin \varphi & \cos \varphi \end{bmatrix} \begin{bmatrix} i_d \\ i_q \end{bmatrix} = C_{2r/2s} \begin{bmatrix} i_d \\ i_q \end{bmatrix} \quad (9)$$

In formula (9), φ is the angle between the d axis of the d-q coordinate system and the axis of the coordinate system, ω ($\varphi = \omega t$) is the rotational angular velocity of the d-q rotating coordinate system. $C_{2r/2s}$ is the transformation matrix from two-phase rotation to two-phase stationary coordinate system.

$$C_{2r/2s} = \begin{bmatrix} \cos \varphi & -\sin \varphi \\ \sin \varphi & \cos \varphi \end{bmatrix} \quad (10)$$

Inverse transformation of equation (3) can get the transformation matrix from two-phase static to two-phase rotation

$$C_{2s/2r} = C_{2r/2s}^{-1} = \begin{bmatrix} \cos \varphi & \sin \varphi \\ -\sin \varphi & \cos \varphi \end{bmatrix} \quad (11)$$

2.1.3 Transformation between three-phase stationary coordinate system and two-phase rotating coordinate system

After obtaining the transformation matrix of the three-phase stationary coordinate system to the two-phase stationary coordinate system and the transformation matrix of the two-phase stationary to two-phase rotation, it can also get the transformation from three-phase stationary coordinate system to two-phase arbitrary rotating coordinate system.

$$\begin{bmatrix} i_a \\ i_\beta \\ i_0 \end{bmatrix} = C_{2s/2r} \begin{bmatrix} i_a \\ i_\beta \\ i_0 \end{bmatrix} = C_{2s/2r} C_{3s/2s} \begin{bmatrix} i_A \\ i_B \\ i_C \end{bmatrix} = C_{3s/2r} \begin{bmatrix} i_A \\ i_B \\ i_C \end{bmatrix} \quad (12)$$

The transformation matrix from the three-phase stationary coordinate system to the two-phase arbitrary rotating coordinate system is

$$\sqrt{\frac{2}{3}} \begin{bmatrix} \cos \varphi & \cos(\varphi - 120^\circ) & \cos(\varphi + 120^\circ) \\ -\sin \varphi & -\sin(\varphi - 120^\circ) & -\sin(\varphi + 120^\circ) \\ \frac{1}{\sqrt{2}} & \frac{1}{\sqrt{2}} & \frac{1}{\sqrt{2}} \end{bmatrix} \quad (13)$$

The transformation matrix from the two-phase arbitrary rotating coordinate system to the three-phase stationary coordinate system is

$$C_{2/3s} = C_{3/2r}^{-1} = \sqrt{\frac{2}{3}} \begin{bmatrix} \cos \varphi & -\sin \varphi & \frac{1}{\sqrt{2}} \\ \cos(\varphi - 120^\circ) & -\sin(\varphi - 120^\circ) & \frac{1}{\sqrt{2}} \\ \cos(\varphi + 120^\circ) & -\sin(\varphi + 120^\circ) & \frac{1}{\sqrt{2}} \end{bmatrix}$$

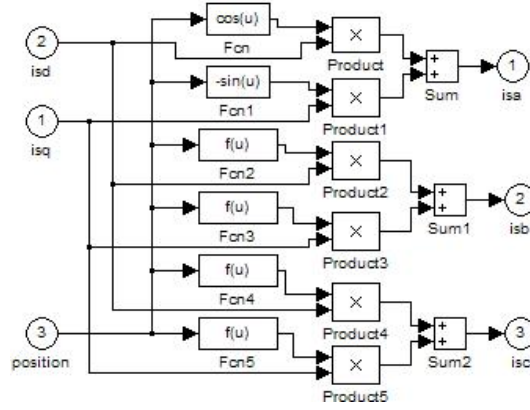


Fig 1Coordinate transformation simulation diagram

2.1.4 Under the dq coordinate system, the motor model

In the d-q coordinate system, the basic formula of asynchronous motor can be obtained:

$$Te = n_p \frac{Lm}{Lr} (i_{sq} \psi_{rd} - i_{sd} \psi_{rq}) \quad (15)$$

$$Te - T_L = \frac{J}{n_p} \frac{d\omega_r}{dt} \quad (16)$$

$$i_{sd} = \frac{U_{sd}}{L_{sc}s + R_s} - \psi_{rd} \frac{1}{L_r} \frac{L_m s}{L_{sc}s + R_s} \quad (17)$$

$$i_{sq} = \frac{U_{sq}}{L_{sc}s + R_s} - \psi_{rq} \frac{1}{L_r} \frac{L_m s}{L_{sc}s + R_s} \quad (18)$$

$$\psi_{rd} = \frac{1}{R_r + L_r s} (i_{sd} L_m R_r - \omega_r L_r \psi_{rq}) \quad (19)$$

$$\psi_{rq} = \frac{1}{R_r + L_r s} (i_{sq} L_m R_r + \omega_r L_r \psi_{rd}) \quad (20)$$

From (15) to (20), the following motor models can be built:

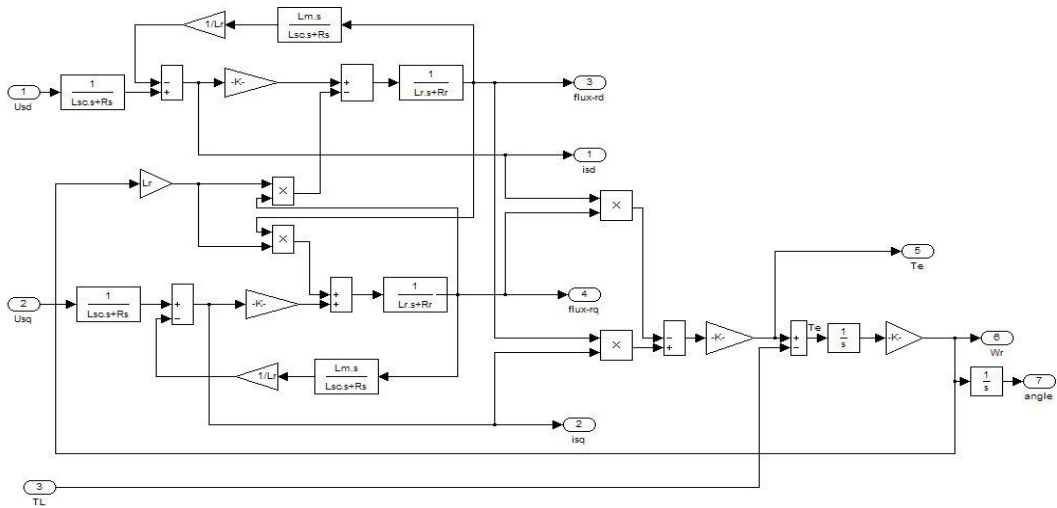


Fig 2 Asynchronous motor simulation model

2.1.5 Establish the entire system simulation model

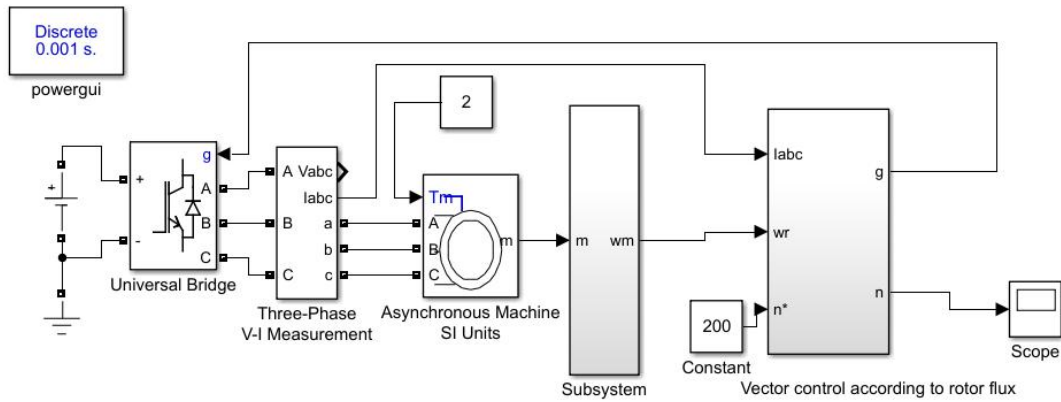


Fig3 System simulation model

2.2 Drive system identification

2.2.1 Principles of system identification

System identification is based on the input and output signals of the system to determine the mathematical model that describes the behavior of the system^[5]. It can get a description of the system through the processing and calculation of input-output (causal) signals. For manual control in industrial processes, the process operator needs to know how the process output responds to different control behaviors. System identification is to study how to obtain the mathematical model of the system from the measured values. According to professional terminology, Zadeh once gave a definition of system identification: System identification is based on input and output, determine a system (model) that is equivalent to the measured system under a certain criterion from a specific type of system (model).

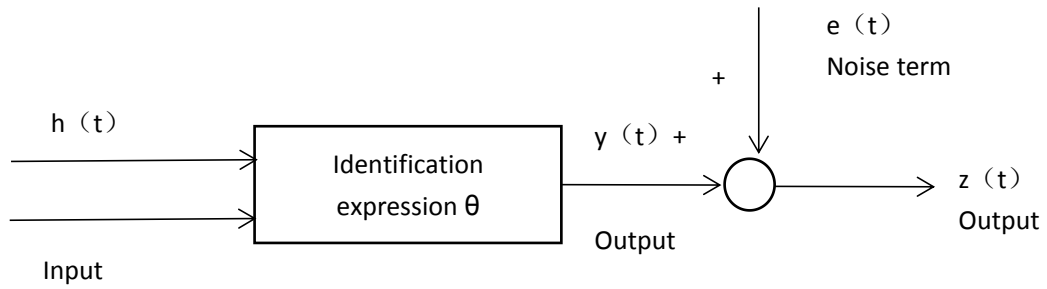


Fig 4 Expressions to identify problems

The system identification method is to identify the transfer function of the system by collecting the input and output signals of the system. The process expression of the control system is:

$$y^n(t) + a_1 y^{(n-1)}(t) + \dots + a_n y(t) = b_0 u^m(t) + b_1 u^{(m-1)}(t) + \dots + b_m u(t)$$

among them, $y(t), u(t)$ is the output and input signal in the time domain, n is the system order of the model, $a_1, \dots, a_n, b_0, \dots, b_m$ is constant, the above formula is transformed by Laplace, we can get a general expression in the time domain of the transfer function

$$G(s) = \frac{Y(s)}{U(s)} = \frac{b_0 s^m + b_1 s^{m-1} + \dots + b_m}{s^n + a_1 s^{n-1} + \dots + a_n}$$

$Y(s), U(s)$ is the output input signal. In the study of system identification, discrete time models are often used for analysis, we introduce unit forward operator and unit delay operator, Get a description of the discrete process of the system.

$$y(t) = G(q)u(t)$$

Pass operator $G(q)$ expression is:

$$G(q) = \frac{b_1 q^{-1} + \dots + b_n q^{-n}}{1 + a_1 q^{-1} + \dots + a_n q^{-n}}$$

2.2.2 System identification steps

Generally speaking, the system identification process includes the following basic steps:

(1) Identification experiment

Reference^[6] uses Chirp signal as excitation signal to study the identification of electro-hydraulic servo system. Reference^[7] used the GBN signal as the excitation signal to

study the rehabilitation exoskeleton robotic arm. Select the generalized binary noise (GBN) signal as the input signal, the selection of sampling time should refer to the response speed of the system, the disturbance and control signals are determined by the bandwidth of the system process. This article selects GBN signal as the excitation signal, GBN signal application and large industrial environment, The choice of time should refer to the response speed of the system, the disturbance and control signals are determined by the bandwidth of the system process. The GBN signal is a randomly generated noise signal, Suitable for control identification experiments related to industrial processes, the generation rule of this signal is that the value of $u(t)$ is switched back and forth between the constant $\pm a$, and switch at a certain conversion moment, meet the following formula with the conversion time t .

$$P[u(t)=-u(t-1)]=P_{sw}$$

$$P[u(t)=u(t-1)]=1-P_{sw}$$

P_{sw} is the conversion probability, That is the probability of the signal switching at each conversion time, each time is distributed independently. therefore, The expectation of the GBN signal is zero.

(2) Model order / Structure selection

Choose the optimal model order, the finalized model can best describe the system under test. In the system identification research, different transfer function models are selected for different measured objects to carry out experimental design. Generally speaking, The models commonly used in system identification are the most commonly used ARX (noisy autoregressive) models, ARMAX (noisy autoregressive moving average) models, GLS (generalized least squares) models, etc. These models are selected for different system structures, the ARX and ARMAX models are used in common systems. In this paper, the ARX model is selected as the system identification model.

(3) Parameter Estimation

Use the optimization algorithm to get the best parameter estimate.

(4) Model checking

For different recognition situations, Determine different accuracy standards, Perform accuracy test on the obtained model, If the accuracy does not meet the requirements, then optimize the previous experimental steps, do the model test again, until it meets the

standard. The test method adopted in this article is 0.3 precision test method, That is, 0.3 times the size of the performance degradation evaluation interval is greater than or equal to the identification parameter error.

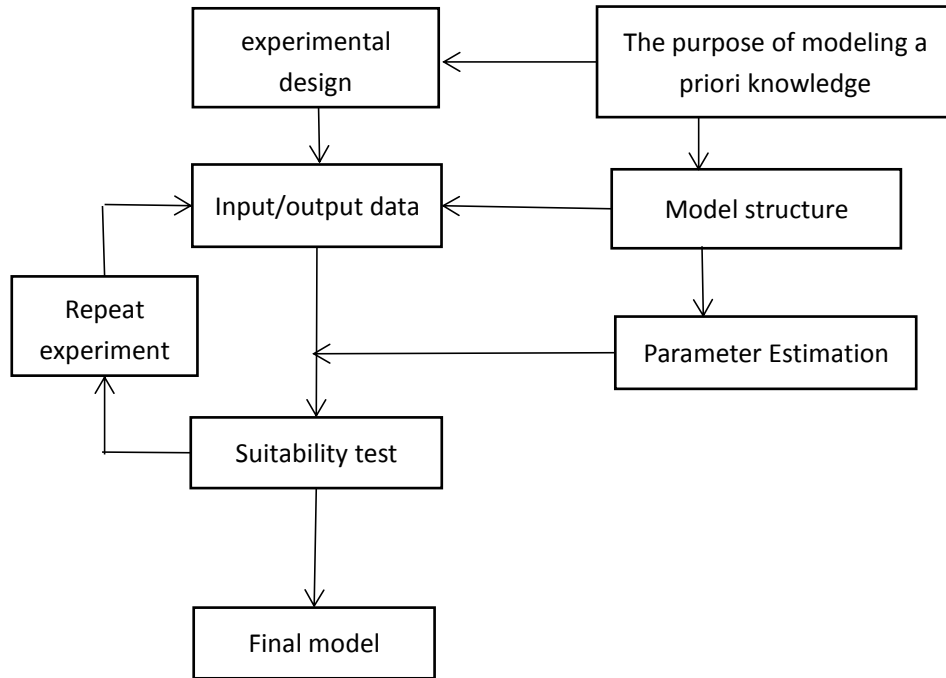


Fig5 Identification process block diagram

2.2.3 Determination of system performance evaluation level

According to the literature ^[8], we can know that during the operation of the electric spindle, its running performance will decrease, That is, the overall performance gradually decreases. In order to make the different results obtained by the system identification have different measurement standards, we need to rank the evaluation results in advance, determine the status of different levels.

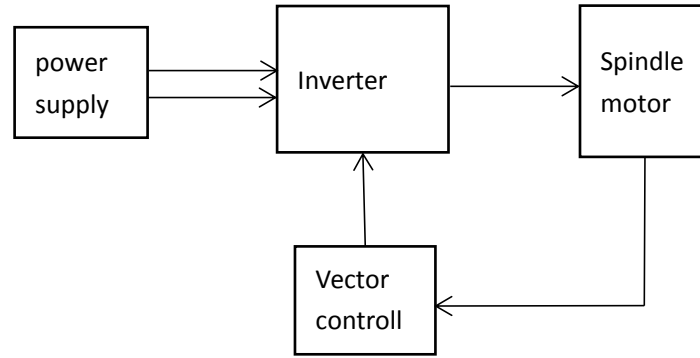


Fig 6 High-speed electric spindle drive system block diagram

This paper determines the degree of performance degradation based on the geometric distance between the parameters identified by the system and the identification parameters of the normal system, the geometric distance (g) reflects the degree of deviation of the values^[9], the evaluation value is obtained by normalizing the calculated distance.

$$g = \sqrt{(x_1 - y_1)^2 + (x_2 - y_2)^2 + \dots + (x_n - y_n)^2} = \sqrt{\sum_{i=1}^n (x_i - y_i)^2}$$

$$x = \frac{g - g_{\min}}{g_{\max} - g_{\min}}$$

Establish four performance evaluation levels between normal and faulty systems, On the basis of summarizing the current classification, this article, this paper proposes a model table for the evaluation of high-speed electric spindle drive system1-1^[10].

table1 Evaluation grade division of drive system

Evaluation level	Evaluation value	Recommended measures
excellent	$0 \leq x < 0.25$	Excellent performance
good	$0.25 \leq x < 0.5$	Normal maintenance
average	$0.5 \leq x < 0.75$	Strengthen maintenance and local repair
poor	$0.75 \leq x \leq 1$	Overhaul

3. IGBT degradation performance evaluation example analysis

3.1 IGBT performance degradation principle

The performance of IGBT is degraded during use,^[11] analyze the degradation process from its internal chip and external package. In terms of internal chips, One is the aging of the solder layer, The solder layer is used to fix the IGBT chip and the package shell, the shell temperature cycle rises and falls, It causes electrothermal shock to the solder layer, leads to fatigue degradation of the solder layer, reduce the heat dissipation capacity of IGBT, causes the junction temperature to rise continuously as the degree of degradation deepens, eventually fails and a short circuit or open circuit fault occurs. The second is that the bonding wire falls

off,The IGBT module continuously withstands the impact of temperature fluctuations during the work process, resulting in the accumulation of plastic strain at the connection point between the bonding wire and the silicon chip, and the cracks at the edge of the connection point between the bonding wire and the chip initially appear.Under the repeated impact of temperature fluctuations,the crack gradually expands, accelerating the fall of the bonding wire,At the same time, the aluminum substrate of the emitter is restructured, which leads to the degradation of IGBT performance.Literature^[12]through temperature cycle experiments,After the device failed, the phenomenon of bond wire shedding, cracking and metal reconstruction was observed through scanning electron microscope pictures.After the performance of the IGBT chip is degraded, the results of bond wire drop and metal reconstruction are shown in Figure 2.2:(a)bond wire off、 (b)bond wire cracks、 (c)the surface of the aluminum substrate without reconstruction before use 、 (d)after the performance degradation and reconstruction, the surface of the aluminum substrate.

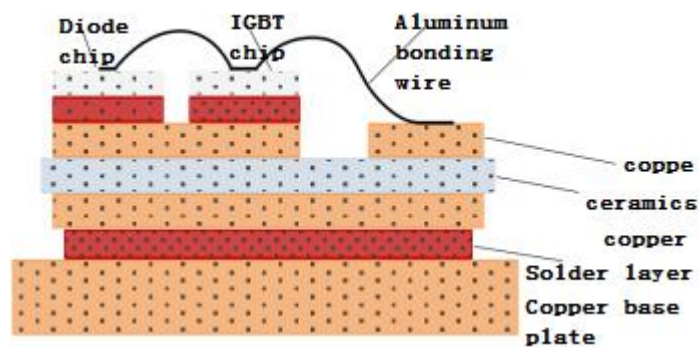


Fig 7 Picture of IGBT device structure degradation

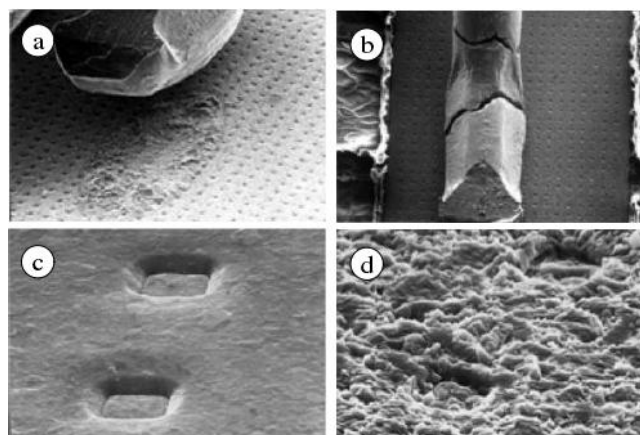


Fig 8 IGBT structure diagram

In terms of the material composition of the package,There are various materials in the packaged IGBT.From Figure 2.1,the material will expand and contract due to temperature changes,Under equal pressure (P-fixed) conditions,Measured by the change in volume of the

material caused by the change in unit temperature, This change can be called the coefficient of thermal expansion (CTE) [13].

Table2 CTE coefficient of each material in IGBT package structure

name	Materials used	Thermal expansion coefficient (ppm/°C)
Aluminum bonding wire	aluminum	22
IGBT chip	silicon	3
Welding layer	Solder	28
ceramics	ceramics	7
Substrate	copper	17.5

The connection between the IGBT chip and the diode chip is made of aluminum metal layer and bonding wire, Moreover, the chip material silicon and the metal layer and the material of the bonding wire have a large difference in thermal expansion coefficient, resulting in the thermal cycling process, Repetitive mechanical stresses caused by different degrees of expansion on the contact surface, This will lead to continuous fatigue degradation of the lead metal layer and the bonding wire subjected to this repeated stress impact.

There are two forms of failure caused by this degradation. One form of failure is to cause reconstruction of the surface of the lead metal layer, On the one hand, the resistance of this part is increased, the power generated is increased, and the junction temperature is further increased, On the other hand, reducing the heat dissipation capability also makes the junction temperature further increase. When the junction temperature is greater than a certain threshold, the parasitic crystal tube in the IGBT is turned on, the gate loses control, and a collector-emitter short circuit occurs; Another type of failure is to cause the bonding wire to break, and an open collector-emitter circuit will occur. The breaking of the bonding wire will also cause the resistance of this part to increase. In summary, Both the lead metal layer and the bonding wire will increase the resistance of this part, Both resistances are part of the resistance of the IGBT collector-emitter channel. therefore, On-line monitoring of the resistance of the IGBT collector-emitter channel enables monitoring of the degree of degradation of the IGBT lead metal layer and bonding wire.

3.2 Performance evaluation of IGBT performance degradation process

3.2.1 IGBT performance degradation simulation design

According to the analysis of the degradation mechanism of IGBT, there are two types of IGBT degradation, bond wire breakage and aluminum metal layer damage. The two forms of degradation eventually lead to an increase in the internal resistance R_{on} , and the internal resistance of the IGBT varies from 0.105 to 0.115. The resistance change inside the IGBT can characterize the degradation degree of the aluminum metal layer and the bonding wire inside

the IGBT, and not affected by changes in load current I_c . Through this part of the analysis, simulation experiments of performance degradation can be established. In the simulation, the value of internal resistance R_{on} is continuously increased to simulate the degradation process of IGBT performance. Set the R_{on} value to 0.110 to evaluate the performance of the current state.

3.2.2 Performance evaluation

The parameters of the asynchronous motor model are set as: rated power $P_N = 20KW$, rated voltage $U_N = 350V$, rated frequency $f_N = 500HZ$, stator resistance $R_s = 0.11\Omega$, rotor resistance $R_r = 0.21\Omega$, stator leakage inductance $L_s = 0.00030239H$, rotor inductance $L_r = 0.00030876H$, stator and rotor mutual inductance $L_r = 0.0086H$, number of pole pairs $p_n = 2$, moment of inertia $J = 0.01kg \cdot m^2$.

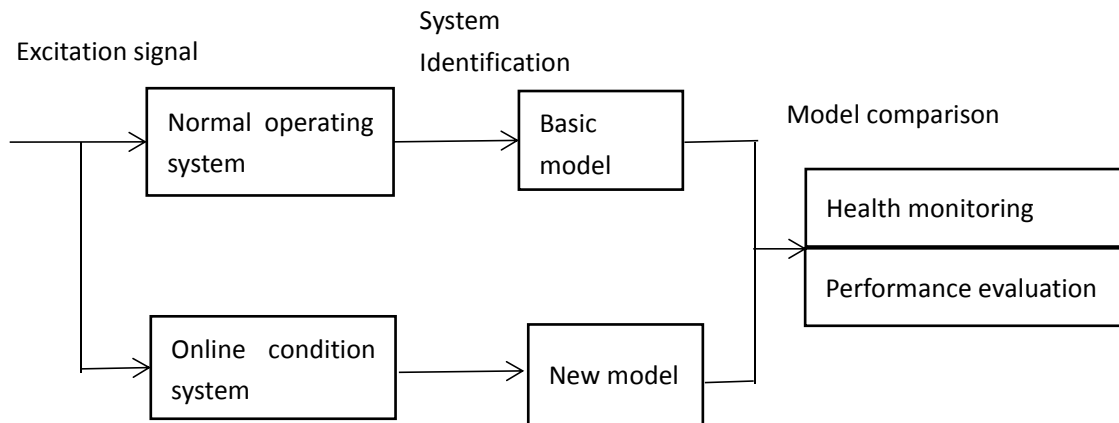


Fig 9 Performance evaluation method based on system identification

When the internal resistance of the IGBT is set to 0.110, according to the theoretical analysis, the evaluation grade of IGBT is good. The identification parameters can be obtained through the system identification method as shown in Table 3.

Fig 10 Identification transfer function table

G_{normal}	$\frac{-0.7136z^{-1} - 0.1279z^{-2}}{1 + 0.3247z^{-1} + 0.2312z^{-2}}$
$G_{R_{on}=0.110}$	$\frac{-0.7113z^{-1} - 0.1051z^{-2}}{1 + 0.3035z^{-1} + 0.2335z^{-2}}$
G_{fault}	$\frac{-0.6712z^{-1} - 0.0763z^{-2}}{1 + 0.2521z^{-1} + 0.2310z^{-2}}$
Performance evaluation	X=0.317, according to the performance evaluation level model table, the performance level is good

The above examples of IGBT degradation confirm the correctness of the established model and system identification performance evaluation method, using the system identification parameter mapping mechanism to evaluate the performance of the system provides a great help to the system performance evaluation.

4 .Conclusion

In this paper, the geometric distance between the identification parameters of the high-speed electric spindle drive system and the normal working system in the actual working process is obtained. Determine the degree of system performance degradation through the geometric distance, the corresponding evaluation level is given to the current system performance. Using this method, an example of IGBT device performance degradation is analyzed. The result shows, The method can evaluate the performance of IGBT degradation process well, The degree of degradation is mapped through the identification parameters. There are few studies using this method to evaluate system performance. The system performance evaluation method based on system identification parameter changes and geometric distance determination lays the foundation for future system performance evaluation research, but a lot of research needs to be further developed.

References

- [1]Luo Yinsheng, Chen Jiazhao.Application of AHP-FCE in mechanical system performance evaluation[J]. Mechanical Manufacturing and Automation,2009,38(03):112-114.
- [2]Tian Qihua,Du Yixian.Research on performance evaluation of mechanical products based on entropy weight fuzzy comprehensive evaluation method[J].China Manufacturing Informatization,2004(03):97-99.
- [3]Abolfazl Simorgh,Abolhassan Razminia,Vladimir I. Shiryaev. System identification and control design of a nonlinear continuously stirred tank reactor[J]. Elsevier B.V.,2020,173.
- [4]Chen Xiaolan, Kang Huimin, He Ye, Chen Man, Miao Yingyun, Chen Wenqu.Analysis of dynamic performance of high-speed electric spindle under speed sensorless vector control[J].Journal of Mechanical Engineering,2010,46(07):96-101.
- [5]Wang-Ji Yan,Meng-Yun Zhao,Qian Sun,Wei-Xin Ren. Transmissibility-based system identification for structural health Monitoring: Fundamentals, approaches, and applications[J]. Mechanical Systems and Signal Processing,2019,117.
- [6]Wang Han, Zhang Maorui, Li Junfu, Du Jing.Chirp signal excited electro-hydraulic servo system identification[J].Machine Tool and Hydraulics,2016,44(13):128-131.
- [7]Gu Wen. Dynamic process health monitoring and diagnosis based on system identification [D]. Zhejiang University,2019.
- [8]Guo Lei, Chen Jin, Zhao Fagang, Dong Guangming, Wang Guowei. Application of geometric distance method based on support vector machine in equipment performance degradation evaluation[J].Journal of Shanghai Jiaotong University,2008(07):1077-1080.
- [9]Yang Bin. Reliability evaluation of electric spindle based on performance degradation[D]. Jilin University,2018.
- [10]Wang Xiaoqiang, Niu Liyong, Huang Yu, Jiang Jiuchun.Electric and safety performance evaluation system of electric vehicle chargers[J].Power Technology,2014,38(04):734-736+744.
- [11]Du Yi, Li Fan, Zeng Zhaoyang, Zheng Jifei. Research on the construction method of IGBT performance degradation model[J]. Power Electronics Technology,2013,47(01):104-106.
- [12]Smet V, Forest F, Huselstein J J, et al. Ageing and Failure Modes of IGBT Modules in High-Temperature Power Cycling[J]. IEEE Transactions on Industrial Electronics, 2011, 58(10):4931-4941.
- [13]Liu Dan.On-line monitoring of IGBT degradation under repeated overcurrent impacts[D]. Zhejiang University,2016.